Gravity-Sensitive Quantum Dynamics in Cold Atoms

Z.-Y. Ma,[1] M. B. d'Arcy,[2] and S. A. Gardiner[3]

[1]*Clarendon Laboratory, Department of Physics, University of Oxford, Oxford OX1 3PU, United Kingdom*
[2]*Atomic Physics Division, National Institute of Standards and Technology, Gaithersburg, Maryland 20899-8424, USA*
[3]*JILA, University of Colorado and National Institute of Standards and Technology, Boulder, Colorado 80309-0440, USA*

(Received 10 November 2003; revised manuscript received 24 June 2004; published 12 October 2004)

We subject a falling cloud of cold cesium atoms to periodic kicks from a sinusoidal potential created by a vertical standing wave of laser light. By controllably accelerating the potential, we show quantum accelerator mode dynamics to be highly sensitive to the effective gravitational acceleration when close to specific, resonant values. This quantum sensitivity to a control parameter is reminiscent of that associated with classical chaos and promises techniques for precision measurement.

DOI: 10.1103/PhysRevLett.93.164101 PACS numbers: 05.45.Mt, 03.65.Sq, 32.80.Lg, 42.50.Vk

The identification and observation of signatures of chaos in quantum dynamics is the goal of considerable current effort. Much of this work centers on the theoretical characterization of energy spectra [1], or such quantities as the Loschmidt echo [2] and fidelity [3], which develop the idea that sensitivity of a wave function's evolution to small variations in a system's Hamiltonian be used as a definition of quantum instability [1–4]. Such quantities could be observed experimentally but require some interpretation to highlight the way in which their nature betokens stability or chaos. An alternative would be the observation of different motional regimes. This is more in sympathy with techniques and philosophy used to identify classical chaos and is the approach used here.

In certain systems the decay of the overlap of two initially identical wave functions evolving under slightly differing Hamiltonians can be expressed in the long time limit as the sum of two decays, governed by Fermi's golden rule and the classical Lyapunov exponent [2]. The decay rate serves as a quantum signature of instability, which can be compared with that of the corresponding classical system. Such sensitivity can be probed interferometrically [5,6]. In the quantum system presented here, the classical limit of which is chaotic, extreme sensitivity of the qualitative nature of the motional dynamics to a control parameter is directly observable. It is manifested by the effect on quantum accelerator mode (QAM) dynamics [6–10] of small variations in the effective value of gravity in the δ-kicked accelerator [7,11]. The QAMs observed in this atom-optical realization [6–10] are characterized by a momentum transfer, linear with kick number, to a substantial fraction (up to $\sim$20%) of the initial cloud of atoms. This is due to a resonant rephasing effect, dependent on the time-interval between kicks, for certain wave functions [9,12]. The sensitivity in the dynamics we observe also promises the capability of precisely calibrating a relationship between the local gravitational acceleration and h/m, where m is the atomic mass, and we describe how our observations constitute a feasibility demonstration of such a measurement.

The Hamiltonian of the δ-kicked accelerator, realized using a magneto-optic trap (MOT) of laser-cooled atoms that are then released and subjected to pulses from a standing wave of off-resonant light, is

$$\hat{H} = \frac{\hat{p}^2}{2m} + mg\hat{z} - \hbar\phi_d[1 + \cos(G\hat{z})] \sum_{n=-\infty}^{\infty} \delta(t - nT), \tag{1}$$

where $\hat{z}$ is the position, $\hat{p}$ is the momentum, m is the particle mass, t is the time, T is the pulse period, $\hbar\phi_d$ quantifies the strength of the kicking potential, $G = 2\pi/\lambda_{\text{spat}}$, and λ_{spat} is the spatial period of the standing wave applied to the atoms. The quantity g is normally the gravitational acceleration; by "accelerating" the standing wave, it is possible to effectively modify g [7,13].

In an analysis by Fishman, Guarneri, and Rebuzzini [12], the fact that QAMs are observed only when T approaches $\ell T_{1/2} = \ell 2\pi m/\hbar G^2$, where $\ell \in \mathbb{Z}^+$ and $T_{1/2}$ is the half-Talbot time [9], is exploited to yield a simplified picture of QAM dynamics. In a frame accelerating with g, the linear potential is removed to leave a spatially periodic Hamiltonian. The quasimomentum β is then conserved, i.e., if a momentum state $|p\rangle = |(k + \beta)\hbar G\rangle$, where $k \in \mathbb{Z}$ and $\beta \in [0, 1)$, "ladders" of momentum states of different β evolve *independently*. The resulting kick-to-kick time evolution operator is

$$\hat{F}_n(\beta) = \exp(-i\{\hat{\rho} + \text{sgn}(\epsilon)[\pi\ell + \tilde{k}\beta - \gamma(n - 1/2)]\}^2/2\epsilon) \exp(i\tilde{k}\cos\hat{\chi}/|\epsilon|), \tag{2}$$

where $\tilde{k} = |\epsilon|\phi_d$, $\tilde{k} = 2\pi T/T_{1/2}$, and $\gamma = gGT^2$. We have introduced $\epsilon = 2\pi(T/T_{1/2} - \ell)$ to quantify the closeness of T to $\ell T_{1/2}$ and the dynamical variables are now an angle $\hat{\chi} = G\hat{z}$ and a discrete conjugate momentum $\hat{\rho} = |\epsilon|(\hat{p}/\hbar G - \beta)$, such that $[\hat{\chi}, \hat{\rho}] = i|\epsilon|$. If one constructs a kick-to-kick Heisenberg map corresponding to Eq. (2) for the dynamical variables, then in the limit $\epsilon \to 0$, the commutator vanishes, and the operators can be replaced by their mean values. Thus

$$\tilde{\rho}_{n+1} = \tilde{\rho}_n - \tilde{k}\sin(\chi_n) - \mathrm{sgn}(\epsilon)\gamma, \quad (3a)$$

$$\chi_{n+1} = \chi_n + \mathrm{sgn}(\epsilon)\tilde{\rho}_{n+1}, \quad (3b)$$

where $\chi_n = \langle\hat{\chi}_n\rangle$, $\tilde{\rho}_n = \langle\hat{\rho}_n\rangle + \mathrm{sgn}[\pi\ell + \hbar\beta - \gamma(n - 1/2)]$. Quantum accelerator modes correspond to stable periodic orbits of this map [6,8,12]. Note that $\epsilon \to 0$ coincides with $\hbar \to 0$ only if $\ell = 0$. Otherwise, as here, the classical-particle-like behavior of QAMs is due to a quantum resonance effect.

Stable periodic orbits yielded by Eq. (3) (and hence QAMs) are classified by order $\mathfrak{p}$ and jumping index $\mathfrak{j}$ (the number of momentum units, in terms of the size of the phase-space cell, traversed after $\mathfrak{p}$ iterations). The sign of $\mathfrak{j}$ is determined by the jumping direction. A necessary condition [12] for the existence of a periodic orbit is $|\mathfrak{j}/\mathfrak{p} + \mathrm{sgn}(\epsilon)\gamma/2\pi| \le \tilde{k}/2\pi$, which can be rewritten (for small ϵ) as

$$-|\epsilon|\left(\frac{\phi_d}{2\pi} + \frac{2\ell\gamma}{\hbar^2}\right) \le \frac{\mathfrak{j}}{\mathfrak{p}} + \mathrm{sgn}(\epsilon)2\pi\ell^2\frac{\gamma}{\hbar^2} \le |\epsilon|\left(\frac{\phi_d}{2\pi} - \frac{2\ell\gamma}{\hbar^2}\right). \quad (4)$$

Both ϕ_d and $\gamma/\hbar^2 = gm^2/\hbar^2G^3$ are independent of T, and therefore of ϵ. Equation (4) is convenient when T is varied from below to above $\ell T_{1/2}$, i.e., scanning ϵ from negative to positive. As $\epsilon \to 0$, the QAMs that occur must be characterized by $\mathfrak{j}$ and $\mathfrak{p}$ such that $\mathfrak{j}/\mathfrak{p} \to -\mathrm{sgn}(\epsilon)2\pi\ell^2\gamma/\hbar^2$. In general $2\pi\ell^2\gamma/\hbar^2$ is an irrational value, and one observes increasingly high-order QAMs as $T \to \ell T_{1/2}$ [8]. If we tune g so that $2\pi\ell^2\gamma/\hbar^2 = r/s$, where r and s are integers, then $\mathfrak{j}/\mathfrak{p} + \mathrm{sgn}(\epsilon)2\pi\ell^2\gamma/\hbar^2 = 0$ for $\mathfrak{j}/\mathfrak{p} = -\mathrm{sgn}(\epsilon)r/s$. Once the $(\mathfrak{p}, \mathfrak{j})$ QAM satisfying this condition appears, shifting T closer to $\ell T_{1/2}$ does not produce higher-order QAMs.

In a frame accelerating with g, the momentum after N kicks, for an initial condition near a $(\mathfrak{p}, \mathfrak{j})$ stable periodic orbit [12], in "grating recoils" $\hbar G$ [9] is

$$q_N \simeq q_0 + N\frac{2\pi}{|\epsilon|}\left[\frac{\mathfrak{j}}{\mathfrak{p}} + \mathrm{sgn}(\epsilon)\frac{\gamma}{2\pi}\right], \quad (5)$$

where q_0 is the initial momentum. We now consider the momentum of orbits specified by $\mathfrak{j}/\mathfrak{p} = r/s$ (for $\epsilon < 0$) and $\mathfrak{j}/\mathfrak{p} = -r/s$ (for $\epsilon > 0$) as a single function of N and ϵ, when $2\pi\ell^2\gamma/\hbar^2$ approaches rational values. Letting $2\pi\ell^2\gamma/\hbar^2 = r/s + w\ell^2$, we find

$$q_N \simeq q_0 + N\frac{r}{s}\left(\frac{2}{\ell} + \frac{\epsilon}{2\pi\ell^2}\right) + Nw\left(\frac{2\pi\ell^2}{\epsilon} + 2\ell + \frac{\epsilon}{2\pi}\right). \quad (6)$$

Scanning through ϵ from negative to positive values, one does not generally observe two QAMs of the same $\mathfrak{p}$ and magnitude of $\mathfrak{j}$ (with positive sign for negative ϵ, and negative sign for positive ϵ) [8,14]. However, in the gravity-resonant cases we consider, when $2\pi\ell^2\gamma/\hbar^2$ is close to r/s, we always observe an r/s and then a $-r/s$ QAM as we scan ϵ. This is shown in Fig. 1, where we plot Poincaré sections produced by Eq. (3) for $\gamma = \hbar^2/2\pi = (2\pi + \epsilon)^2/2\pi$ (i.e., $r/s = 1$) and $\tilde{k} = |\epsilon|\phi_d = |\epsilon|0.8\pi$ (the approximate experimental mean value [7]). The islands around the $(\mathfrak{p}, \mathfrak{j}) = [1, -\mathrm{sgn}(\epsilon)1]$ periodic orbits remain large over a wide range of ϵ and, in contrast to Ref. [8], no higher-order island structures appear as $\epsilon \to 0$. In Fig. 2(a) the corresponding QAMs are robust and uninterrupted by higher-order QAMs as $T \to T_{1/2}$.

From Eq. (6) we see that for a given N, q is a linear function of ϵ whenever $w = 0$. If $w \neq 0$ this changes to a hyperbolic function, where the arms of the hyperbolas point in opposite directions for oppositely signed w. Deviation from straight line behavior in a QAM accelerated to a given momentum will be greater for a gravity-resonant mode corresponding to smaller $\mathfrak{j}/\mathfrak{p} = r/s$, since the QAM acceleration is $\propto \mathfrak{j}/\mathfrak{p}$, but the deviation is $\propto N$. We consider only QAMs where $\mathfrak{j} = r = 1$, so high-order modes exhibit, for a given momentum transfer, greater sensitivity to variations in g.

In our realization of the quantum δ-kicked accelerator, $\sim 10^7$ cesium atoms are trapped and cooled in a MOT to 5 μK, yielding a Gaussian momentum distribution of FWHM $6\hbar G$. The atoms are then released and exposed to periodic pulses from a laser standing wave 15 GHz red-detuned from the $6^2S_{1/2} \to 6^2P_{1/2}$ $(F = 4 \to F' = 3)$ D1 transition. Hence the spatial period of the standing wave is $\lambda_{\mathrm{spat}} = 447$ nm, and $T_{1/2} = 66.7$ μs. The peak standing wave intensity is $\simeq 5 \times 10^4$ mW/cm^2, and the pulse duration is $t_p = 500$ ns. This is sufficiently short that the atoms are in the Raman-Nath regime and each pulse

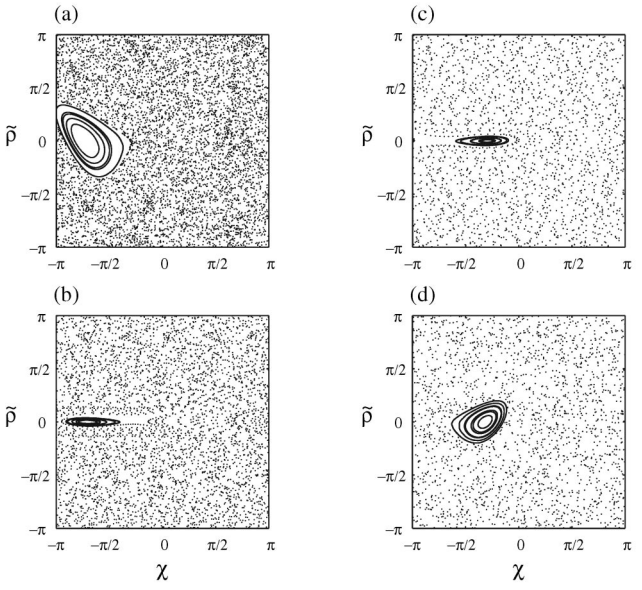

FIG. 1. Phase-space plots for Eq. (3), when $2\pi\gamma/\hbar^2 = 1/1 \Rightarrow \gamma = (2\pi + \epsilon)^2/2\pi$, and $\tilde{k} = |\epsilon|0.8\pi$ for $\epsilon = -0.88$ (a), -0.02 (b), 0.03 (c), and 0.6 (d). This corresponds to $T =$ 57.4, 66.5, 67, and 73 μs. For (a),(b) the island corresponds to a $(\mathfrak{p}, \mathfrak{j}) = (1, 1)$ QAM, and for (c),(d), to a $(\mathfrak{p}, \mathfrak{j}) = (1, -1)$ QAM.

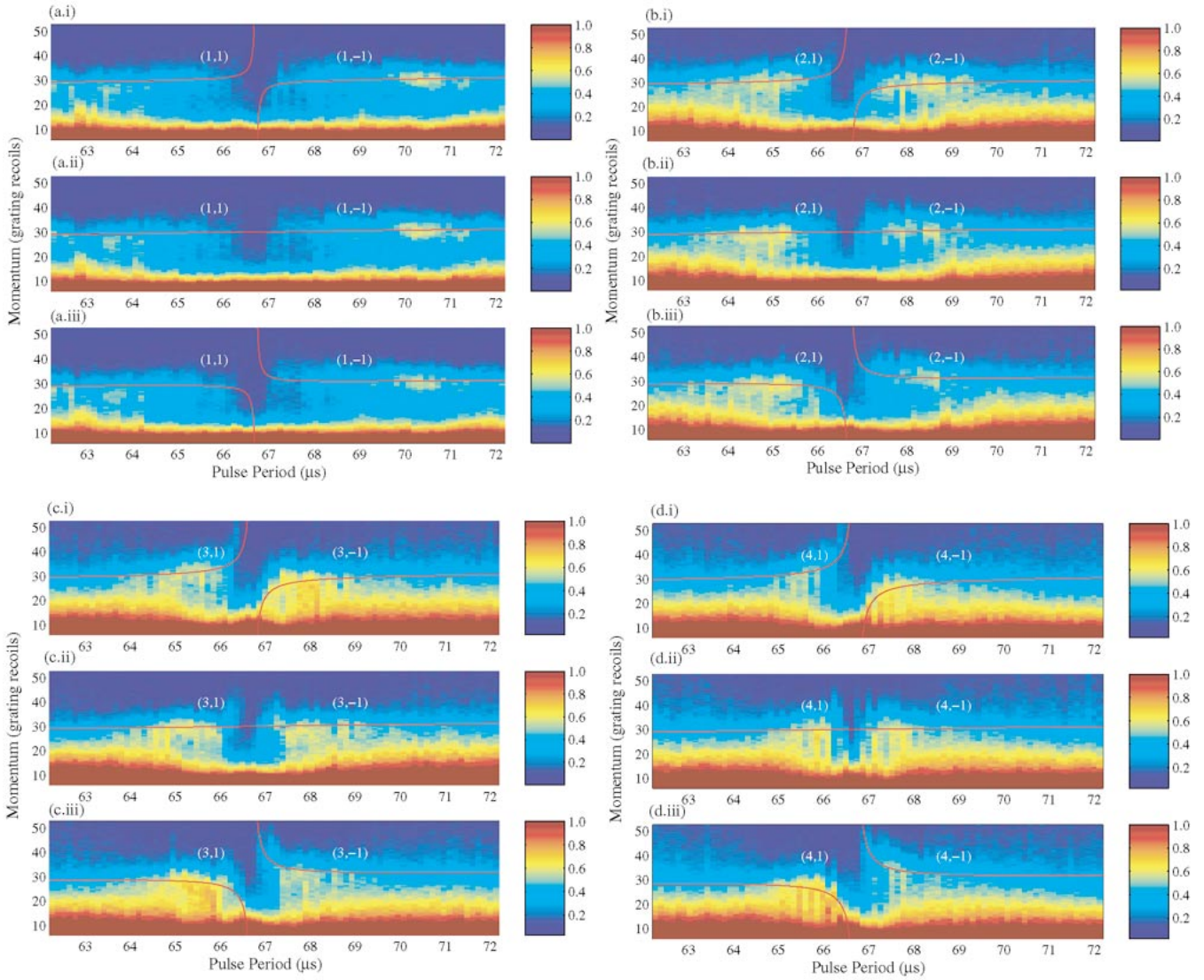

FIG. 2 (color online). Density plots of experimental momentum distributions for different effective gravity g corresponding to (a) $r/s = 1/1$ (after 15 kicks), (b) $r/s = 1/2$ (30 kicks), (c) $r/s = 1/3$ (45 kicks), and (d) $r/s = 1/4$ (60 kicks), as T is varied near the half-Talbot time $T_{1/2} = 66.7$ μs, from 60.5 to 74.5 μs in steps of 0.128 μs. In each case the QAM corresponds to $\dot{\jmath}/\dot{\wp} = r/s$; subplot (i) corresponds to $w \simeq -8.5 \times 10^{-4}$ (deviation from resonant g is $\sim -8.6 \times 10^{-2}$ ms^{-2}), subplot (ii) to $w \simeq 0$, and subplot (iii) to $w \simeq 8.5 \times 10^{-4}$ (deviation from resonant g is $\sim 8.6 \times 10^{-2}$ ms^{-2}). Overlaid lines, labeled $(\dot{\wp}, \dot{\jmath})$, indicate QAM momenta predicted by Eq. (6). Population arbitrarily normalized to maximum value = 1, and momentum defined in a frame falling with g. Note the significantly greater population at high momentum (up to $50\hbar G$) near $T_{1/2}$ in (d)(i) and (d)(iii), compared to (a)(i) and (a)(iii).

approximates a δ-function kick. The potential depth is quantified by $\phi_d = \Omega^2 t_p/8\delta_L$, where Ω is the Rabi frequency and δ_L is the detuning from the D1 transition. During the pulse sequence, a voltage-controlled crystal phase modulator stroboscopically accelerates the standing wave profile. The atoms therefore effectively experience a controllable value of gravity. After the pulsing sequence, the atoms fall through laser light resonant with the $6^2S_{1/2} \rightarrow 6^2P_{3/2}$ ($F = 4 \rightarrow F'' = 5$) D2 transition, 0.5 m below the MOT. By monitoring the absorption, the atoms' momentum distribution is then measured by time of flight, with resolution $\hbar G$ [7,9].

In Fig. 2 we show momentum distributions for experiments in which T was scanned across $T_{1/2}$ from 60.5 to 74.5 μs, with $2\pi\gamma/\hbar^2$ varied in the vicinity of r/s equal to (a) 1/1, (b) 1/2, (c) 1/3, and (d) 1/4. To maintain the ideal ($w = 0$) total momentum transfer, 15, 30, 45, and 60 kicks were applied fixing Nr/s. For each of Figs. 2(a)–2(d) the data displayed are in subplot (ii), $2\pi\gamma/\hbar^2 = r/s$ (as exactly as feasible), yielding a linear variation of the QAM momentum with T; and in subplots (i) and (iii), for equal positive and negative deviations from this near-ideality, yielding hyperbolic variation of the QAM mo-

momentum. Typically ~10%–20% of the atoms populate the QAM.

In each subplot (ii) of Fig. 2, the QAM momentum predicted by Eq. (6) is identical. The expected linear dependence on T appears to be well confirmed by the data, although the separation of the QAM from the non-accelerated cloud, centered at $p = 0$, is clearer for smaller $s = \wp$ (there is less momentum diffusion for fewer kicks). In Fig. 2(a), subplots (i) and (iii) are barely distinguishable from subplot (ii), whereas in Fig. 2(d), the distributions in subplots (i) and (iii) are highly asymmetric compared with subplot (ii), with, close to $T_{1/2}$, noticeable population at up to $50\hbar G$. The asymmetry inverts from below [subplot (i)] to above [subplot (iii)] the resonant value of gravity. We therefore observe a clear qualitative change in the QAM dynamics, highly sensitive to a control parameter. The displayed predictions of Eq. (6) show that deviations from linear behavior occur only when very close to $T_{1/2}$ in Figs. 2(a)(i) and 2(a)(iii), but are much more significant in Figs. 2(d)(i) and 2(d)(iii). This is due to the larger number of kicks necessary for large $s = \wp$ to achieve the same QAM momentum.

The procedure of determining the "standing wave acceleration" at which straight line behavior of a given $(\wp, \jmath)$ QAM momentum is observed as a function of T could, in principle, be used as a sensitive atom-optical means of relating h/m [15] to the local gravitational acceleration [16]. This is because $2\pi\gamma/\hbar k^2 = r/s$ can be rewritten $g = (h/m)^2(r/s)/\lambda_{\text{spat}}^3$ and would be determined by noting when the *total* acceleration (sinusoidal potential plus gravitational) causes these equalities to be fulfilled for a known r/s, and then subtracting the imposed acceleration of the potential. In our setup, where the potential is "accelerated" by using a crystal phase modulator to phase shift the retroreflected laser beam [7,9], the phase shift for a particular applied voltage is difficult to calibrate more precisely than ~1%. This limits the precision in measuring the relationship between the local gravitational acceleration and h/m to ~1%. An accurate prediction of the QAM momenta for imperfectly resonant values of the effective gravity, as displayed in Fig. 2, is also hampered. This could be improved if the moving sinusoidal potential were formed by two counterpropagating beams with a controllable frequency difference [17], where calibration of the phase shift to between 1 ppm and 1 ppb is possible. Calibration of λ_{spat} to less than 1 ppb is also feasible [16], allowing for the possible sensitive determination of either the local gravitational acceleration [16] or h/m [15], depending on which is initially known more precisely. The feasibility of any such scheme will depend on how precisely the atomic ensemble's dynamics permit the determination of the acceleration of the sinusoidal potential for which the resonant, linear with T, behavior of the QAM occurs. Ascertaining this will require substantial theoretical and experimental investigation.

We have observed qualitative changes in the motional quantum dynamics of cold cesium atoms, highly sensitive to the precise value of an externally adjustable parameter, the effective gravity. This is distinct from conceptually related proposals that consider slightly differing Hamiltonians to study the Loschmidt echo or fidelity and demonstrates a link to the concepts of highly sensitive dynamics in classically chaotic systems. We have described a feasible experimental scheme taking advantage of this sensitivity to determine a relationship between the local gravitational acceleration and h/m.

We thank K. Burnett, S. Fishman, I. Guarneri, L. Rebuzzini, G. S. Summy, and particularly R. M. Godun, for very helpful discussions. We acknowledge support from the Clarendon Bursary, the U.K. EPSRC, the Royal Society, the EU through the TMR "Cold Quantum Gases" Network, the Lindemann Trust, and NASA.

[1] F. Haake, *Quantum Signatures of Chaos* (Springer, Berlin, 2001), 2nd ed.
[2] F. M. Cucchietti *et al.*, Phys. Rev. E **65**, 046209 (2002); R. A. Jalabert and H. M. Pastawski, Phys. Rev. Lett. **86**, 2490 (2001).
[3] N. R. Cerruti and S. Tomsovic, Phys. Rev. Lett. **88**, 054103 (2002); Y. S. Weinstein, S. Lloyd, and C. Tsallis, *ibid.* **89**, 214101 (2002); G. Benenti and G. Casati, Phys. Rev. E **65**, 066205 (2002).
[4] A. Peres, *Quantum Theory: Concepts and Methods* (Kluwer Academic Publishers, Dordrecht, 1993).
[5] S. A. Gardiner, J. I. Cirac, and P. Zoller, Phys. Rev. Lett. **79**, 4790 (1997).
[6] S. Schlunk *et al.*, Phys. Rev. Lett. **90**, 054101 (2003).
[7] M. B. d'Arcy *et al.*, Phys. Rev. E **64**, 056233 (2001).
[8] S. Schlunk *et al.*, Phys. Rev. Lett. **90**, 124102 (2003).
[9] R. M. Godun *et al.*, Phys. Rev. A **62**, 013411 (2000).
[10] M. K. Oberthaler *et al.*, Phys. Rev. Lett. **83**, 4447 (1999); M. B. d'Arcy *et al.*, Phys. Rev. A **67**, 023605 (2003).
[11] S. Fishman, in *Quantum Chaos*, edited by G. Casati, I. Guarneri, and U. Smilansky (IOS Press, Amsterdam, 1993); R. Graham, M. Schlautmann, and P. Zoller, Phys. Rev. A **45**, R19 (1992); F. L. Moore *et al.*, Phys. Rev. Lett. **75**, 4598 (1995); H. Ammann *et al.*, *ibid.* **80**, 4111 (1998); P. Szriftgiser *et al.*, *ibid.* **89**, 224101 (2002).
[12] S. Fishman, I. Guarneri, and L. Rebuzzini, Phys. Rev. Lett. **89**, 084101 (2002); J. Stat. Phys. **110**, 911 (2003).
[13] M. B. d'Arcy *et al.*, Phys. Rev. Lett. **87**, 074102 (2001); Phys. Rev. E **69**, 027201 (2004).
[14] The sign of $\jmath$ is consistent with that of the gravitational potential and with the definition of $\jmath$ in Ref. [12].
[15] S. Gupta *et al.*, Phys. Rev. Lett. **89**, 140401 (2002); R. Battesti *et al.*, *ibid.* **92**, 253001 (2004).
[16] A. Peters, K. Y. Chung, and S. Chu, Nature (London) **400**, 849 (1999).
[17] J. Hecker Denschlag *et al.*, J. Phys. B **35**, 3095 (2002).